Optimal Design of a Coupled Photovoltaic-Electrolysis-Battery System for Hydrogen Generation

Aisha Alobaid*[a,b] and Raymond A. Adomaitis[a]

[a] *Department of Chemical and Biomolecular Engineering, Institute for Systems Research, University of Maryland, College Park, MD, 20742, USA*

[b] *Chemical Engineering Department, College of Engineering and Petroleum, Kuwait University, 13060, Kuwait*

Supplementary Material

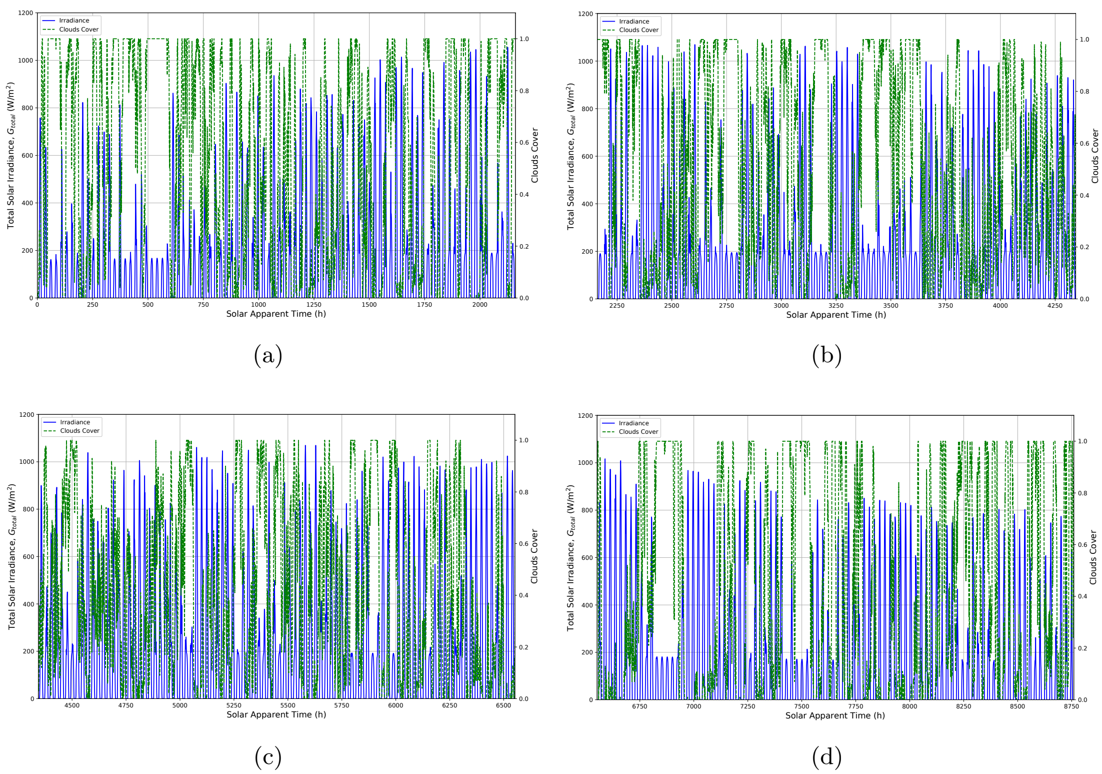

Fig. S1. Hourly cloud cover data from Dark Sky API for College Park, MD and the solar irradiance G_{total} calculated at a module tilt angle of 35° for the year 2017, divided into 4 periods: January, February, March (a) April, May, June (b), July, August, September (c), and October, November, December (d).

*Corresponding author
Email: aisha.alobaid@ku.edu.kw
Address: Chemical Engineering Department, College of Engineering and Petroleum, Kuwait University, P.O.Box 5969, Safat, 13060, Kuwait

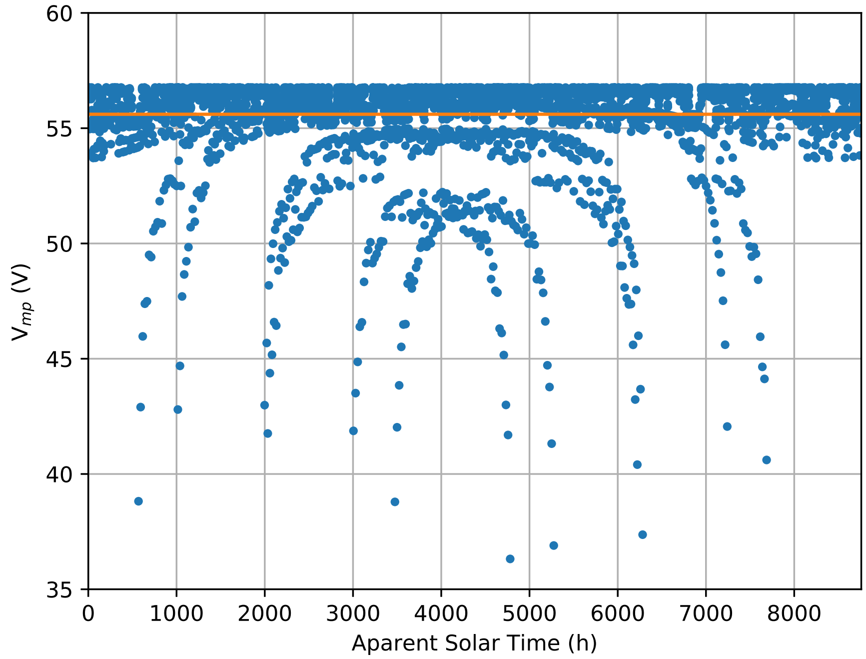

Fig. S2. Non-zero values of the V_{mp} (i.e., during daylight operation of the PV module), with the mean value calculated.

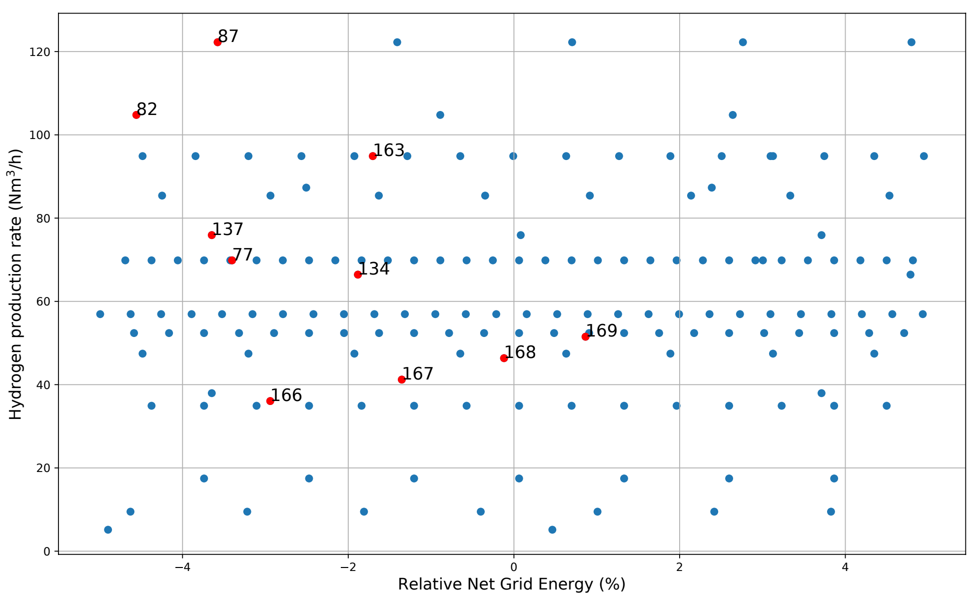

Fig. S3. Hydrogen production rate and the relative net grid energy, showing the 10 Pareto-Frontier points in red.

Table S1. A list of the input parameters and variables used in the model

Input Parameters		Output
	Solar Irradiance Modeling	
$G_{sc} = 1366$	The solar constant (W/m^2)	
$\delta = 23.44°$	Earth's declination at $t_d = 0$	
$n_{ast} = 24$	Number of intervals within a day	
i	Index in range n_{ast} ($i = 0$ to $n_{ast} - 1$) defines the time of the day	• The Global irradiance G_G (W/m^2), Equation (13)
ϕ	Latitude measured north of the equator (°)	• The total solar irradiance G_{total} (W/m^2) , Equation (15)
z	Site elevation (km)	
θ_{tilt}	PV module tilt angle (°)	
$CloudsCover$	Clouds cover (fraction between 0 and 1)	
	PV Module	
I_{ph}	Photo-current (A)	
I_o	Dark saturation current (A)	
R_s	Series resistance (Ω)	
R_{sh}	Shunt resistance (Ω)	• PV module operating current I, Equation (16)
β	Diode ideality factor	
$X(t)$	Dimensionless concentration factor proportional to the global irradiance at time t	• PV modules power P_{pv} (kW), $P_{pv} = M_{pv} \times I_{mp} \times V_{mp}$
V	PV module operating voltage (V)	
M_{pv}	Number of PV modules connected in parallel	
	Electrolyzer	
N	Number of cells connected in series	• Electrolysis Cell current I_{cell} (mA/cm^2), Equation (17) and Fig. 4
M	Number of electrolysis stacks connected in parallel	• Electrolyzer Power P_e (kW), Equation (18)
V_{cell}	Electrlysis cell voltage (V), $V_{cell} = V_{mp}/N$	• Hydrogen Production rate V_{H_2} (Nm^3/h), Equation (20)
	Battery	
η_b	Battery round-trip efficiency (%)	• Battery Energy E_b (kWh), Equation (21)
Cap	Battery capacity (kWh)	
P_{pv}	PV modules power (kW)	• Battery state of charge SOC, Equation (22)
P_e	Power of the Electrolyzer (kW)	
	Economic Model	
U_j	Unit j capital cost ($/kW)	
$U_{\text{O\&M},j}$	Unit j O&M cost ($/kW)	
P_j	Power produced or consumed (kW) in unit j	
n_j	Lifetime of the j^{th} component (years)	• Annual cost of the system ACS ($/yr), Equation (23)
i	Real discount rate	
RF	Replacement cost factor	• Levelized cost of energy LCE ($/kWh), Equation (38)
NGE	Net grid energy (kWh)	
E_{an}	Annual energy produced by the PV system (kWh/yr)	

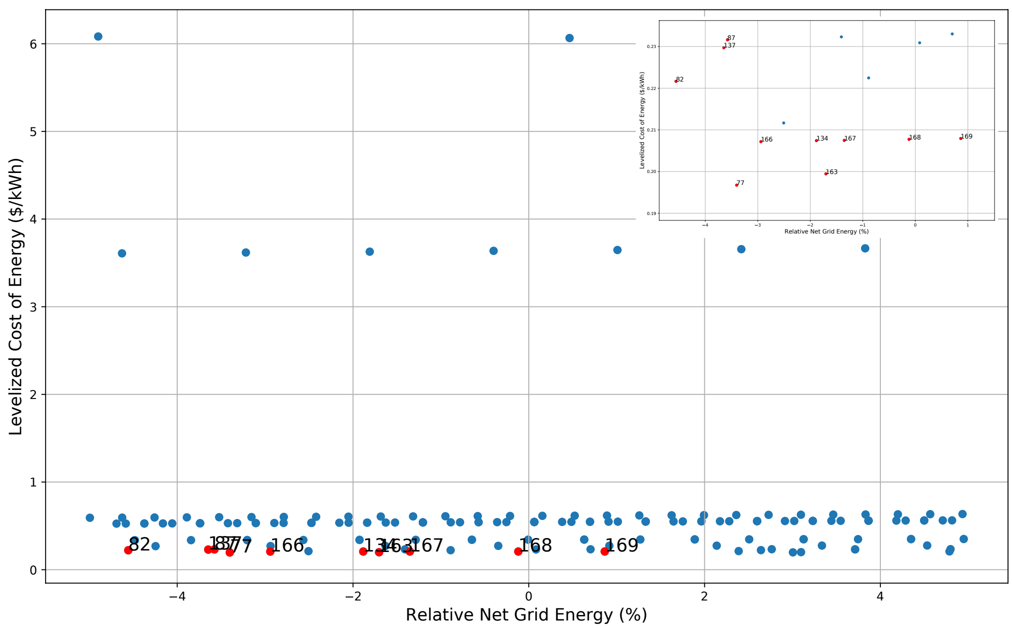

Fig. S4. LCE and the relative net grid energy, showing the 10 Pareto-Frontier points in red.

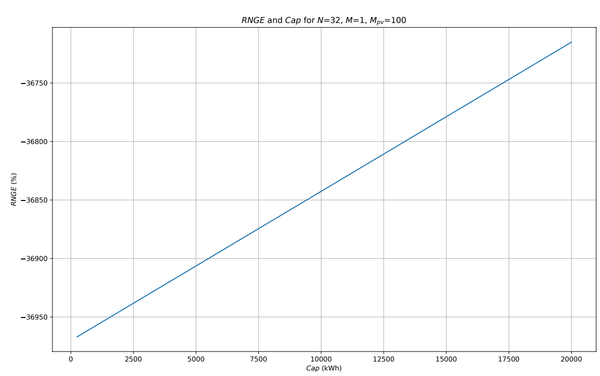

(a)

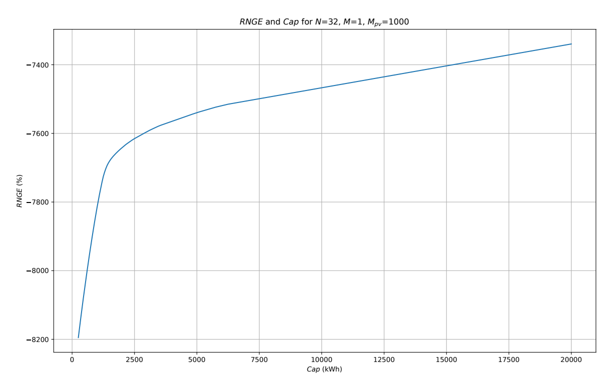

(b)

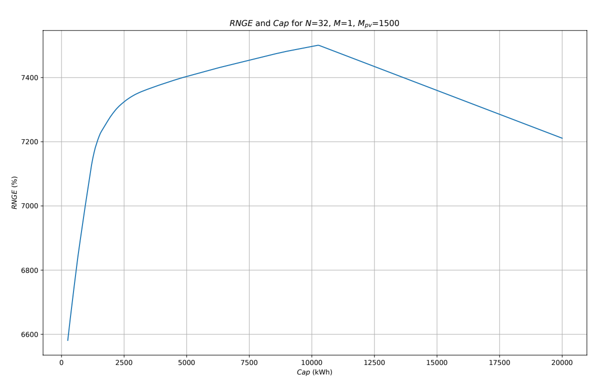

(c)

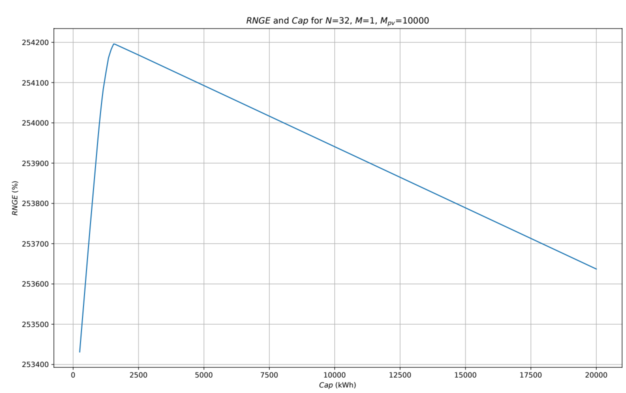

(d)

Fig. S5. Effect of changing the battery capacity at fixed system design, for M_{pv} of 100 (a), 1,000 (b), 1,500 (c), and 10,000 (d).

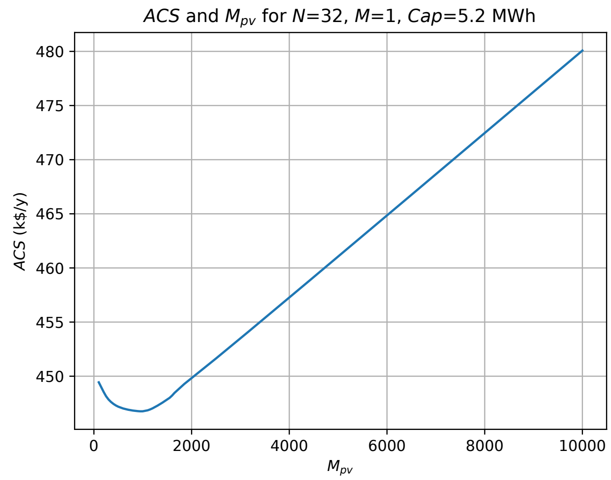

Fig. S6. Effect of number of PV modules M_{pv} on the total annualized system cost ACS.

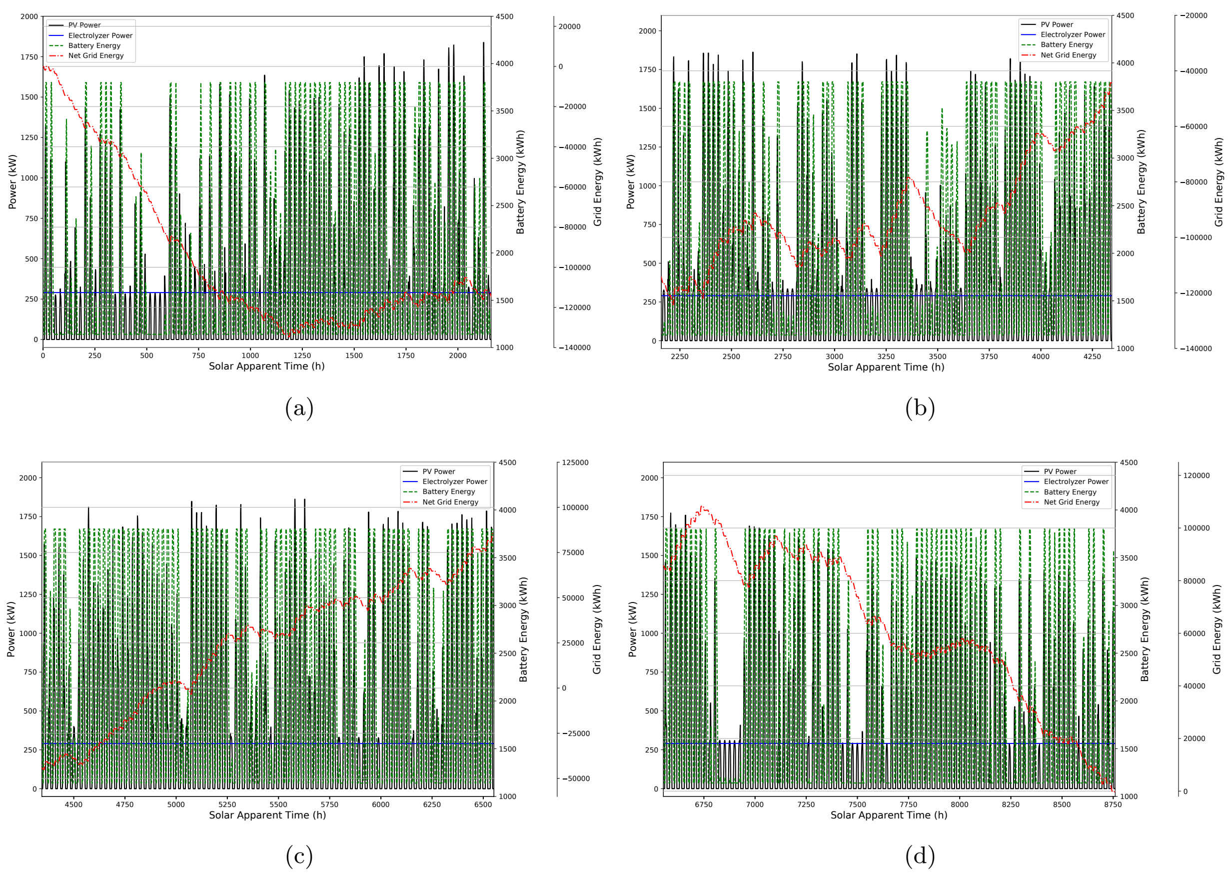

(a) (b) (c) (d)

Fig. S7. Simulation results for point 77 in Table 4 for the year 2017, divided into 4 periods: January, February, March (a) April, May, June (b), July, August, September (c), and October, November, December (d).